Application of Field Modeling Technique on Fire Services Design

W.K. Chow

ABSTRACT

Application of a fire field model on assessing fire services systems is illustrated in this paper. In such an approach, the fire environment is simulated by a set of elliptical partial differential equations describing conservation of mass, momentum, and enthalpy. The airflow, temperature, and smoke concentration contour induced by a fire source is predicted by solving the system of equations numerically using the finite difference method. The predicted result is then used to assess the performance of the longitudinal ventilation in a tunnel, the smoke extraction fans in an atrium building, and the interaction effect between the fire-induced airflow and a sprinkler water spray.

INTRODUCTION

In order to provide guidelines for designing appropriate fire services systems such as detectors, sprinklers, smoke extraction systems in offices, train compartments, atria, or tunnels, it is necessary to know the fire environment that will be encountered in case of accident (Thomas 1981). In the past, this was normally estimated from experience and empirical data on tests of materials or compartmental fires. Statistical analysis on past fire records could also give the risk of a certain building type and, perhaps, the designed fire size. For example, a fire with an area of 3 m by 3 m and heat power of 5 MW is commonly taken as the design value for shopping malls (Morgan 1991). For a better understanding on the fire environment in more complex buildings, fire models, both physical and computational, have to be used (Thomas 1981). Sufficient fire services systems can then be installed. However, performing experiments with physical models would require prohibitive resources. Therefore, apart from extracting relevant empirical data and validating theoretical models, they are not regarded as tools for design purposes. Computer fire models are therefore developed.

There are two types of deterministic models (Galea and Markatos 1987). The first is the zone model, which is a single-compartment approach that assumes the fire is in a room with an environment at certain initial temperature and pressure (Jones 1983). A set of equations incorporating the basic conservation laws of heat and mass can be arrived at by considering the energy flow from the burnt objects and the form in which energy is released. The net energy input to the fire zone by radiation, convection, and conduction is related to all the objects within the zone. Transfer of energy and mass is by convection and radiation due to the fire plume.

The other deterministic model is the field modeling technique (Galea and Markatos 1987); it has developed rapidly as computational fluid dynamics has become more and more popular (Spalding 1980). Although still in the infancy stage, the field modeling technique is believed to be the one with the greatest potential for simulating a fire realistically. Unlike a zone model, only minimal input parameters are required. It is particularly useful for big enclosures, such as atrium buildings or tunnels, where the distribution of temperature is required. This paper illustrates how a fire field model can be applied to simulate fire for different enclosures and evaluate the associated fire services systems. The computer program concerned is run in a VAX minicomputer, but it can be executed successfully, with longer CPU time in small computing systems, such as personal computers for two-dimensional simulation (Dongarra 1987). This is very useful for local building services professionals, as personal computers are commonly installed in most engineering firms.

Building Fire Zone Model

Nearly all zone models divide the burning compartment into two zones: an upper layer containing the hot gases and a lower layer of cool air (Jones 1983, Quintiere 1987) (Figure 1). The set of equations is:

Geometry. The room height H is related to the thickness of the hot gas layer Z_u and cool-air layer Z_l by:

$$H = Z_u + Z_l \tag{2.1}$$

There is a neutral plane where the pressure of the hot layer P_u is equal to that of the cool zone P_l:

$$P_u = P_l \tag{2.2}$$

Conservation of mass. The net rate of mass change in the upper and lower layers M_u and M_l are the sum of the mass lost rate of all the burning objects.

$$\frac{dM_u}{dt} = \sum_i \dot{M}_{i,u} \tag{2.3}$$

W.K. Chow, Principal Lecturer, Department of Building Services Engineering, Hong Kong Polytechnic, Hong Kong.

$$\frac{dM_u}{dt} = \sum_i \dot{M}_{i,u} \qquad (2.4)$$

where $M_{i,u}$ is for the i^{th} object in the upper layer and $M_{i,l}$ is for the i^{th} object in the lower layer.

Conservation of energy. The enthalpy accumulated in the layers is related to temperatures T_u T_l; pressures P_u P_l; velocities V_u V_l; the enthalpy of the i^{th} object $h_{i,u}$, $h_{i,l}$ in the upper and lower layers, respectively; and the heat gained in the upper layer Q_u, specific heat C_p of the gas by:

$$CpM_u \frac{dT_u}{dt} = V_u \frac{dP_u}{dt} + \dot{Q}_u + \sum_i h_{i,u} \dot{M}_{i,u} \qquad (2.5)$$

$$CpM_l \frac{dT_l}{dt} = V_l \frac{dP_l}{dt} + \sum_i h_{i,l} \dot{M}_{i,l} \qquad (2.6)$$

Ideal gas law. The gases are assumed to obey the ideal gas law:

$$P_u = \rho_u R T_u \qquad (2.7)$$

$$P_l = \rho_l R T_l \qquad (2.8)$$

where ρ_u and ρ_l are the densities of the gases in the upper and lower layers, respectively. The heat rate gained at the upper layer $\dot{Q}_u$ in Equation (2.5) describes the heat rate of radiation $\dot{Q}_R$, convection $\dot{Q}_C$, from fire source $\dot{Q}_f$, and objects $\dot{Q}_o$:

$$\dot{Q}_u = \dot{Q}_R + \dot{Q}_C + \dot{Q}_f + \dot{Q}_o \qquad (2.9)$$

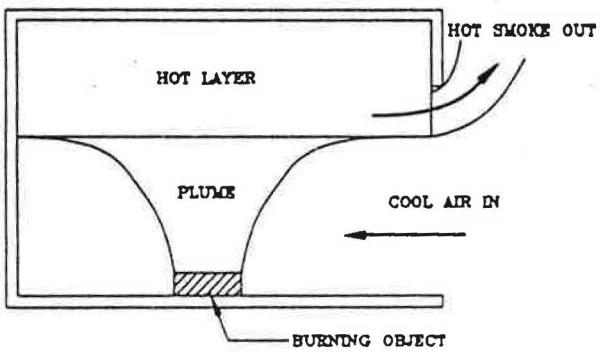

Figure 1 *Configuration for zone model*

The thermal-radiative heat $\dot{Q}_R$ is composed of two parts: heat transfer from hot gases, walls, and surfaces; and radiation transferred from the burning objects and the fire. While the first can be easily computed, the second part is more difficult to predict because the geometry, absorption, and emission coefficients are not well defined. The thermal feedback process makes the situation much more difficult. The thermal convective term $\dot{Q}_C$ is computed by confining to walls inside and outside the room.

Model accuracy depends largely on $\dot{Q}_f$ which, in turn, relies heavily on data from experiments on the fire plume, which is essentially a corkscrewing transfer of mass and energy upward. There are three types of plume: point source (on the fuel surface); area source; and virtual-point source (where the plume size at the fuel surface is equal to that computed for the fire). Many zone models are available in the literature with good experimental support (Cooper 1982, Jones 1983, Quintiere 1987, Mitler and Rockett 1987, Tanaka and Nakamara 1989, Jones and Peacook 1989, Cooper and Forney 1990). All the models require a large volume of empirical input data. The temperature distribution inside the burning enclosure cannot be predicted.

Building Fire Field Model

A building fire field model can simulate the fire-induced field of flow, temperature, and smoke concentrations within an enclosure at the preflashover stage (Galea and Markatos 1987). Current development (Hasemi 1977, Yang and Chang 1977, Liu and Yang 1978, Markatos *et al.* 1982, 1984, 1986, Baum *et al.* 1982, Satoh 1983, Mao *et al* 1984, Kumar and Cox 1985, 1988, Cox 1987, Chow and Leung 1988, 1989, Wichman and Baum 1988, Bos *et al.* 1984, Van de Leur *et al.* 1989) is up to a stage that the flow and temperature field can be predicted successfully by visualizing the fire plume as a heat source described with certain experimentally determined distribution functions. At the moment, this is a natural convection problem that is good for predicting the flow-field driven by buoyancy at a distance from the fire source. The results are good at the preflashover stage or for smoke movement prediction because combustion and thermal radiation are unimportant during the early phase of a fire (Rhodes 1989). It does not account for as many physical processes as a zone model, although it has the potential to extend up to such levels of practicability (but it will take time). Studies on including combustion effects are in progress (Cox 1987, Raycraft *et al.* 1988). The laminar flamelet seems to be capable of giving a more realistic description. However, the present situation will give reasonable results for a building services engineer to design fire systems and for the fire officers to approve the fire safety aspects of building plans.

The flow induced inside an enclosure by a fire source with megawatts of thermal power (such as a burning polyurethane foam sofa) is turbulent. The inertial force due to density differences between hot and ambient air is much greater than the viscous one. This can be justified by the chaotic and random nature of the thermodynamic and hydrodynamic properties of the fluid. Solving the system of equations describing those properties is very difficult. Obviously, there is no analytical solution. Even solving them by computers is not an easy task since the eddies generated might be dissipated to a small size in the magnitude of millimeters.

Fortunately, for engineering application, knowing the averaged values of the air momentum, density, pressure, enthalpy, etc. is good enough (Spalding 1980, Markatos 1986). Any instantaneous value of those physical variables ϕ_t (air velocity, pressure, enthalpy) can be expressed as its average value ϕ plus its fluctuation ϕ' (Spalding 1980):

$$\phi_t = \phi + \phi' \qquad (3.1)$$

The set of equations describing conservation laws on ϕ_t can therefore be transformed into a form in ϕ with

the fluctuation terms ϕ' separated out:

$$\frac{\partial (\rho\phi)}{\partial t} + \text{div}\,[\rho \bar{V} \phi - \Gamma_\phi \text{grad}_\phi] = S_\phi \quad (3.2)$$

where ρ is the air density, and $\bar{V}$ is the velocity vector of airflow.

$$\bar{V} = u\hat{x} + v\hat{y} + w\hat{z} \quad (3.3)$$

Γ_ϕ, S_ϕ are the effective exchange coefficient and the source term for ϕ.

Different turbulent models are proposed to close the above set of equations. In this way, additional equations similar to Equation (3.1) can be derived. But the diffusion coefficient Γ_ϕ will be replaced by an effective value which is much greater than the laminar one. The k-ϵ (Spalding 1980) model is used here to close the set of equations (Chow and Leung 1988, 1989, Chow 1991). The variable ϕ now becomes velocity components, u, v, w, enthalpy h, smoke concentration f, and turbulence parameters k, ϵ. Table 1 gives a summary on ϕ, Γ_ϕ, and S_ϕ.

For solid-wall boundary, the wall function approach is used (Launder and Spalding 1974). The shear stress close to the solid wall is treated as constant, and the velocity parallel to the wall is fitted by a logarithmic function. The near-wall shear stress $t\tau_w$ is given by:

Variable ϕ	Effective Diffusivity Γ_ϕ for ϕ	Source of ϕ: S_ϕ
1	0	0
u	μ_{eff}	$-\frac{\partial p}{\partial x} + \frac{\partial}{\partial x}(\mu_t \frac{\partial u}{\partial x}) + \frac{\partial}{\partial y}(\mu_t \frac{\partial v}{\partial x}) + \frac{\partial}{\partial z}(\mu_t \frac{\partial w}{\partial x})$
v	μ_{eff}	$-\frac{\partial p}{\partial y} - g(\rho - \rho_{eff}) + \frac{\partial}{\partial x}(\mu_t \frac{\partial u}{\partial y}) + \frac{\partial}{\partial y}(\mu_t \frac{\partial v}{\partial y}) + \frac{\partial}{\partial z}(\mu_t \frac{\partial w}{\partial y})$
w	μ_{eff}	$-\frac{\partial p}{\partial z} + \frac{\partial}{\partial x}(\mu_t \frac{\partial u}{\partial z}) + \frac{\partial}{\partial y}(\mu_t \frac{\partial v}{\partial z}) + \frac{\partial}{\partial z}(\mu_t \frac{\partial w}{\partial z})$
f	$\frac{\mu_{eff}}{\sigma_f}$	R_f (In fire plume area)
h	$(\frac{\mu_l}{\sigma_l} + \frac{\mu_t}{\sigma_t})$	$\dot{q}'''$(in fire plume area)
k	$\frac{\mu_{eff}}{\sigma_k}$	$G_k - \rho\epsilon + G_B$
ϵ	$\frac{\mu_{eff}}{\sigma_\epsilon}$	$C_1 \frac{\epsilon}{k}(G_k + G_B)(1 + C_3 R_f) - C_2 \rho \frac{\epsilon^2}{k}$

with μ_l : Laminar viscosity of air

$$\mu_t = C_D \frac{\phi k^2}{\epsilon}$$

$$\mu_{eff} = \mu_l + \mu_l$$

G_k, G_B are the complicated terms in the k-ϵ model

C_1, C_2, C_3 are the empirical coefficients

R_f : Richardson flux number

ϕ_l, ϕ_t, ϕ_f, ϕ_h, ϕ_k, ϕ_ϵ : Prandt numbers

$$\tau_w = \frac{\rho_p K C_D^{1/4} k_p^{1/2} u_p}{\ln (E\ Y+)} \qquad (3.4)$$

where:

$$Y+ = \frac{y_p C_D^{1/4} \rho_p k_p^{1/2}}{\mu_l} \qquad (3.5)$$

Equation (3.4) will be used later in other source terms such as that for k in the near-wall treatment. The velocity components parallel to the wall are computed under the no-slip condition. The one perpendicular to the wall is obtained by setting the adjacent node inside the wall to zero. At the free boundary, the derivatives of the flow quantities are taken to be zero.

For the enthalpy equation, the adiabatic wall condition is applied at the near-wall grid node.

$$\int_0^{y_p} \varepsilon dy = (\sqrt{C_D}\, k_p)^{1.5} \frac{1}{K} \ln (EY+) \qquad (3.6)$$

The near-wall dissipation ϵ_p can be computed directly from

$$\varepsilon_p = \frac{C_D^{3/4} k_p^{3/2}}{K y_p} \qquad (3.7)$$

The set of equations given by Equation (3.1) is discretized into finite difference forms by integrating over the control volume elements divided in the enclosure, as shown in Figure 2 (Patankar 1980). The field variable ϕ at time t at the grid node P can be expressed in terms of ϕ at its neighbors (*i.e.*, X+, X−, N, S, E, W):

$$a_p \phi_p = a_{X+} \phi_{X+} + a_{X-} \phi_{X-} + a_N \phi_N + a_S \phi_S + a_E \phi_E + a_W \phi_W + b \qquad (3.8)$$

where the coefficients a_p, a_{X+}, a_{X-}, a_N, a_S, a_E, and a_W are shown in Appendix A.

The numerical scheme employed here is the SIMPLER (Semi-Implicit Method for Pressure-Linked Equations Revised) (Patankar 1980). This procedure is found to be applicable for both three-dimensional parabolic and elliptic flows problems. Further, the under-relaxation technique is used to ensure computational stability. Details have been described elsewhere and will not be repeated here (Chow and Leung 1988, 1989).

Numerical Experiments

For illustrating the application of a field model to fire services design, numerical experiments are performed to simulate the following examples:

Tunnel

An interesting area is the fire services design, especially the fire ventilation system for vehicular or underground railway tunnels. The case considered in this paper is a tunnel 390 m in length, 5 m in width, and 5.7 m in height, with a false ceiling for accommodating air

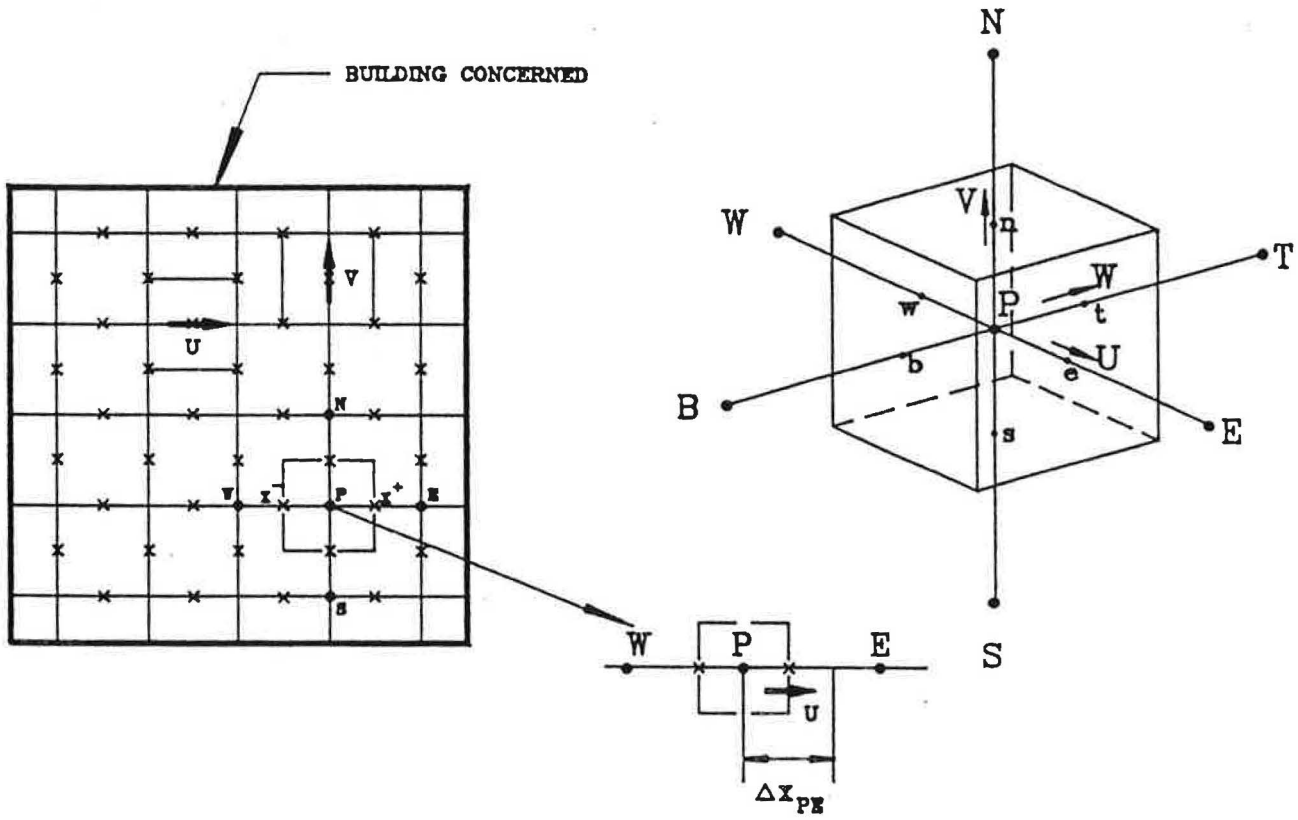

Figure 2 *Grid nodes for field model*

ducts located at a height of 4 m. The schematic plan of the tunnel is shown in Figure 3.

A nonuniform rectangular grid system is used in this three-dimensional simulation program (Chow and Leung 1988). The number of grid lines along x (*i.e.*, the length), y (*i.e.*, the height), and z (*i.e.*, the width) are 85, 12, and 14, respectively. They represent a total of 14,280 grid nodes. The ignition source is located 108 m away from the closed wall. Its output power increases linearly from 0 to 7.225 MW in 10 s. In the simulation, it is assumed that the smoke has the same density as air and is produced uniformly at a rate of 61,400 ppm per second over a volume of 13.44 m around the source after a time of 10 s. The predicted results are shown in Figure 4. Only the section near the ignition source is reported. This region extends over a distance of 20 m, in which the fire source is located near the center. At the initial state, a symmetric flow field that associates with a strong convection current can be seen around the fire source. The velocity of the uprising current is increased to about 10 ms^{-1} when the fire reaches its full strength. The buoyancy effect generates a hot air layer which finally propagates outwards to form a ceiling jet. The jet plays an important role in transferring heat to those areas far from the ignition sources. The maximum jet velocity is about 7 ms^{-1}. Smoke particles are carried away by the moving stream along the

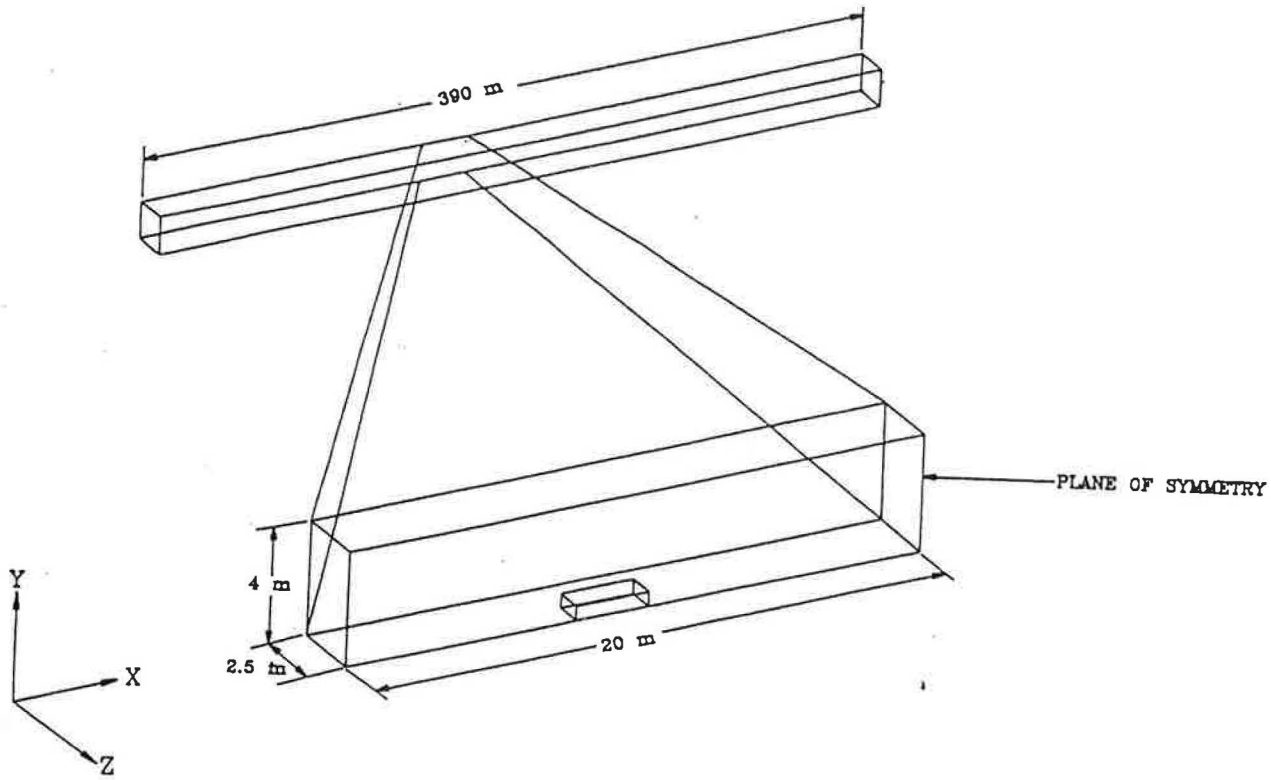

Figure 3 *Tunnel segment with fire source*

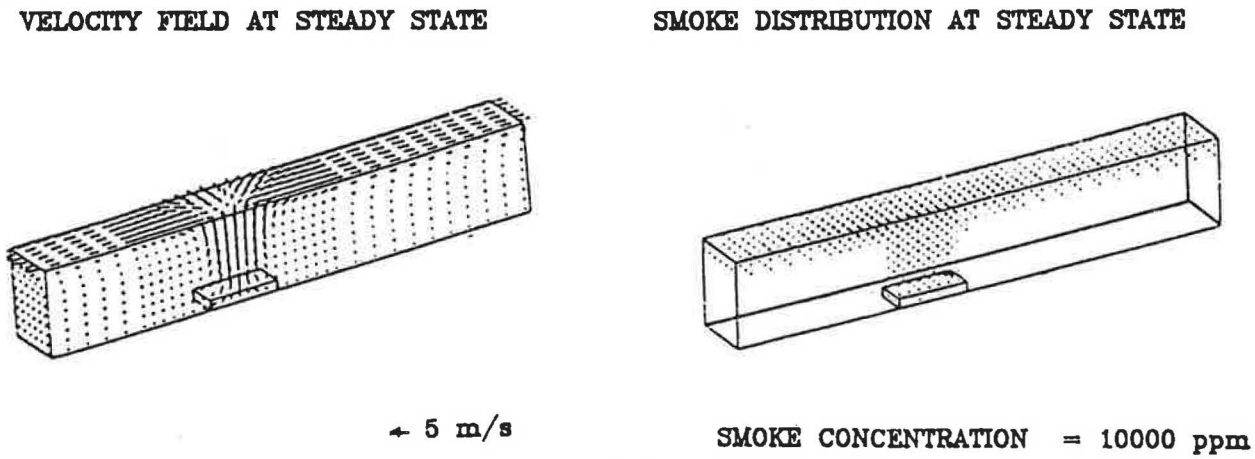

Figure 4 *Velocity field and smoke distribution with natural ventilation*

ceiling. The spreading of smoke is illustrated clearly on the 3-dimensional diagrams in Figures 4 to 6.

To demonstrate the effect of longitudinal ventilation on confining a tunnel fire, the wall boundary condition at the left terminal is replaced by introducing a constant velocity component (*i.e.*, the ventilation stream velocity) along x direction to the velocity grid nodes. In addition, a positive gage pressure should also be imposed on the pressure grid node just outside the terminal. This is referred to as a continuous injection of fresh air into the tunnel cavity. The ventilation system will be activated at 30 s after ignition.

The effects of forced ventilation on the flow field are illustrated in Figures 5 and 6, where both the flow fields and smoke movement patterns are shown. In the first trial, the impressed air velocity is set at 4 ms^{-1}, corresponding to a mass flow rate of 96 kgs^{-1}. At about 1 min after activating the ventilation system, the inflow air arrives at the ignition source. It interacts with the ceiling jet and generates a vortex with a linear dimension of about 3 m near the head of the fire plume. It has been reported that if the impressed airspeed is low, hot air may flow opposite to the applied air direction. This is known as back layering. Whether this will occur or not depends on a number of factors, including the thermal power of the fire source, the geometry of the tunnel, and the ventilation speed. The critical velocity V_c of the ventilation air to prevent the back-layering effect can be estimated from the following equations (Thomas 1970):

$$V_c = 0.61 \left(\frac{gHQ}{\rho_\infty C_p A T_f}\right)^{1/3} \tag{3.9}$$

$$T_f = \frac{Q}{\rho_\infty C_p A V_c} + T_\infty \tag{3.10}$$

where g, Q, C_p, ρ, T_∞, A, and H represent the acceleration due to gravity, power of heat source, specific heat of air at constant pressure, ambient air density, hot gas temperature, cross-sectional area, and height of the tunnel. Substituting numerical data for this example, *i.e.*, Q = 7.225 MW, C = 1100 J $kg^{-1}K^{-1}$, ρ = 1.21 kgm^{-3}, A = 10 m^2, H = 4 m, and the ambient temperature T_∞ is chosen as 290K; the corresponding critical velocity is estimated to be 2.5 ms^{-1}. Therefore, using 4 ms^{-1} obviously exceeds the initial values and will be effective in confining the fires. But a value smaller than 2.5 ms^{-1} is

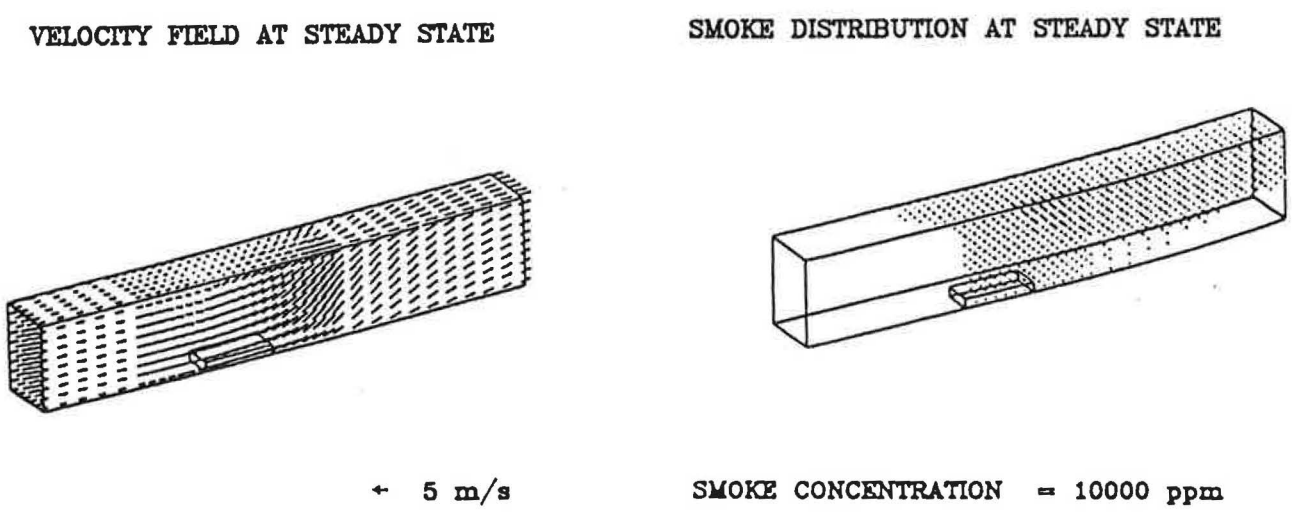

Figure 5 *Velocity field and smoke distribution with longitudinal ventilation 4 m/s*

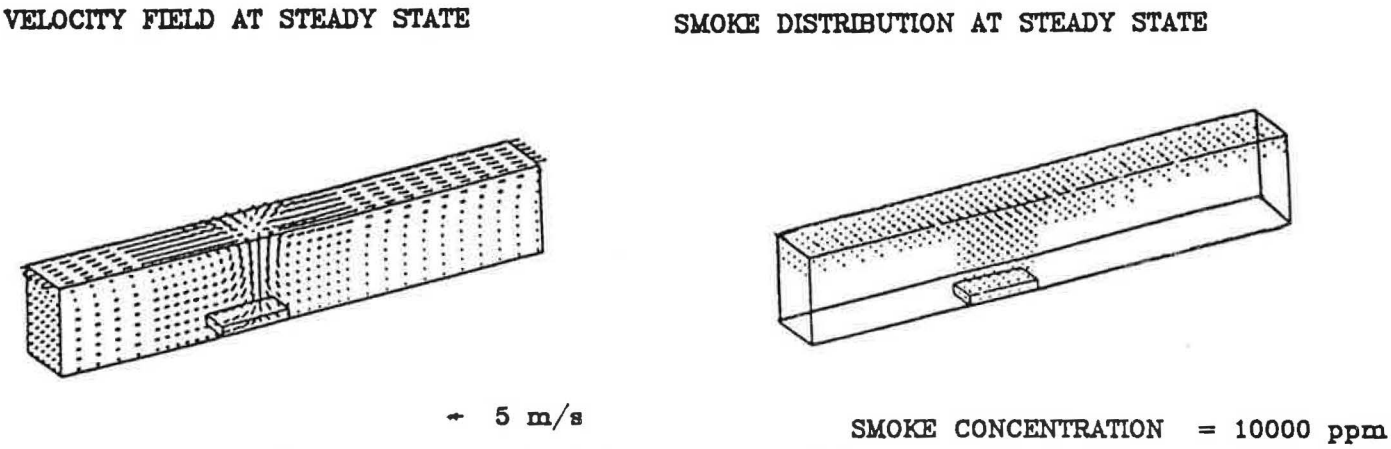

Figure 6 *Velocity field and smoke distribution with longitudinal ventilation 1.5 m/s*

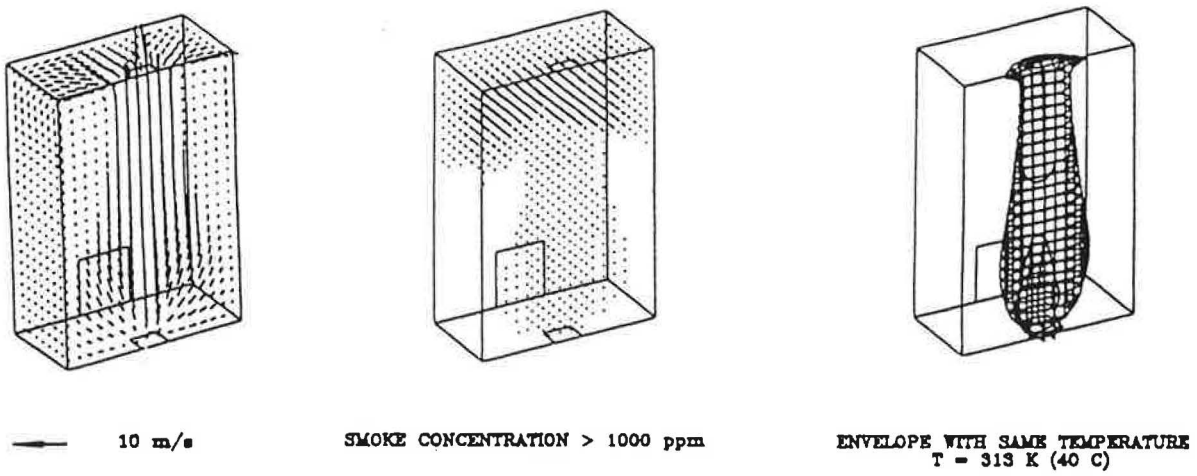

Figure 9 *Flow field, smoke, and temperature distribution for atrium under forced ventilation*

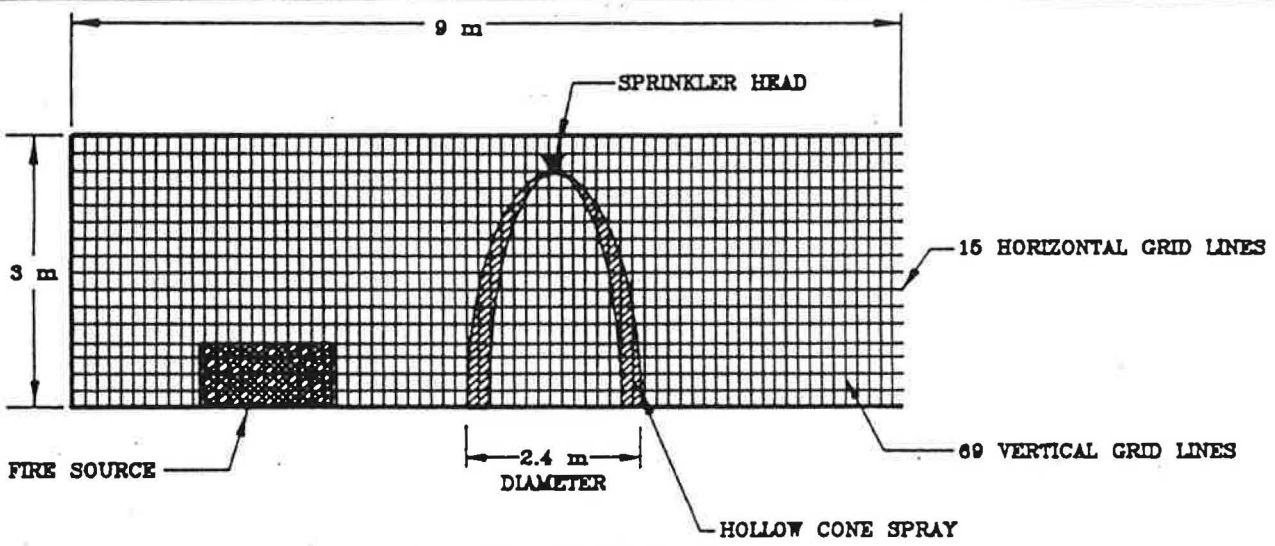

Figure 10 *Sprinklered building*

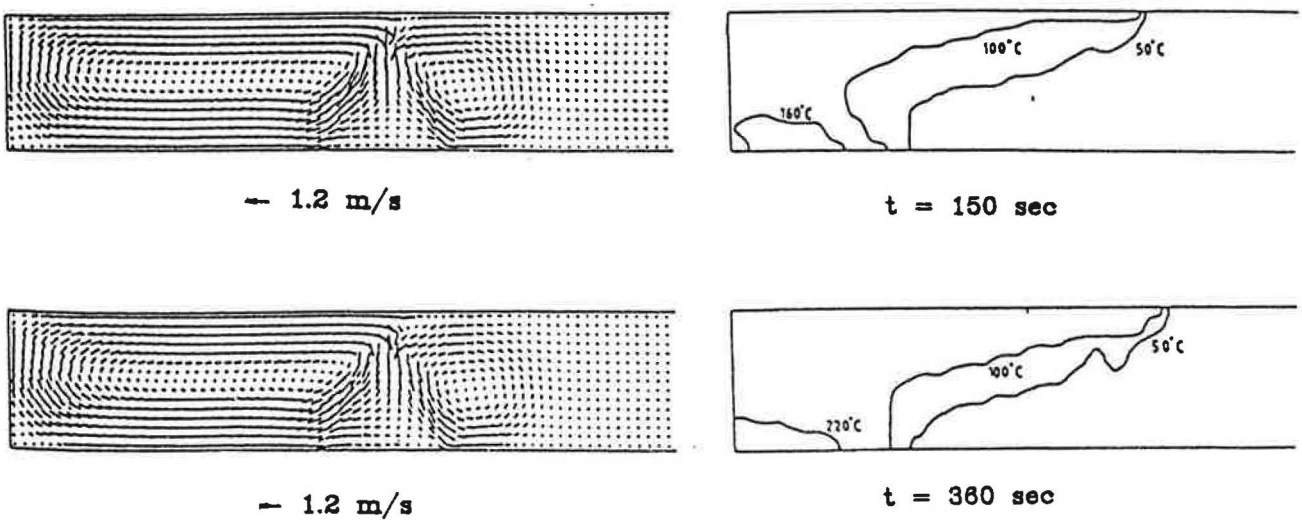

Figure 11 *Temperature and flow field for a sprinklered fire*

not able to prevent the back-layering effect. To illustrate this, a lower ventilating speed of 1.5 ms^{-1} is used. Now, only the flow field near the bottom of the fire plume is slightly disturbed. The reverse flow near the ceiling cannot be suppressed, as is clearly shown in Figure 6.

Atrium Building

Application of field model to atrium fire services design is an important area to be developed (Waters 1989, Chow and Leung 1989 a and b, Porter 1990). An atrium building of dimensions 16 m x 16 m x 24 m is considered in this paper. A square vent of area 6.25 m^2 is located at the center of the roof, at which free boundary conditions are applied. There are two doorways 4.5 m in width and 5 m in height located in the opposite side walls (Figure 7) (Chow and Leung 1989). A fire of size 2 m by 4 m and a constant heat release rate of 5.0 MW is located at the center of the floor. The smoke-generating rate is 0.7266 kgs^{-1}. The initial temperature and pressure are

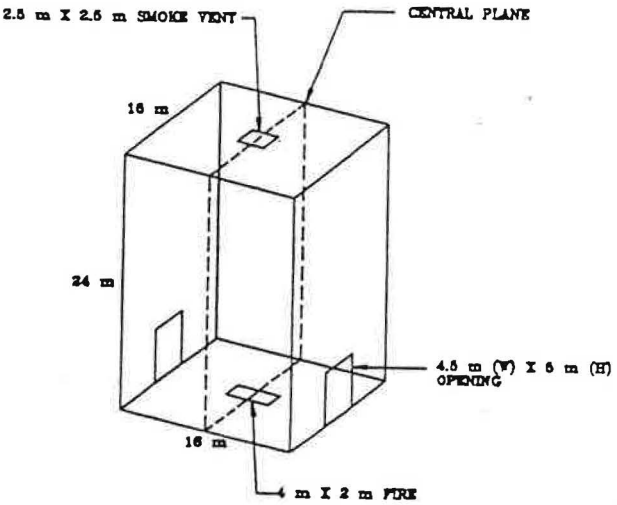

Note: Since the system is symmetrical about the central plane, only half the atrium was simulated so as to save computational effort.

Figure 7 *Atrium building*

17°C and 101,325 Pa, respectively. After ignition, a strong uprising hot stream is found near the fire source. Heat is transferred to the surroundings by convection, and a hot gas cloud therefore grows rapidly around the fire. Although the vent can be served as an exit for the smoke, a large quantity of smoke returns to the building interior. As a result, the upper part of the building is heated. The results for steady flow and temperature are given in Figure 8.

From this computational result, natural venting may not be effective in extracting smoke from the burning atrium and a mechanical system is recommended. To evaluate its performance, a negative gage pressure of 400 Pa is imposed on the pressure grid nodes just outside the openings. In addition, the vertical velocity component at the openings is set to be 10 ms^{-1}, which represents the installation of an exhaust fan at the ceiling openings. Figure 9 shows that the amount of smoke returned to the building is greatly reduced. The temperature inside the building is lowered, and the possibility of smoke particles returning to the building interior is further reduced.

Sprinkler Induced Airflow

Another area in which the field model may be applied is the study of the effect of sprinkler water sprays on the fire-induced airflow (Chow and Fong 1990). With it, the smoke logging effect can be studied (Morgan 1979). The physical layout of the building in question is shown in Figure 10. A wooden crib fire source with a height of 0.8 m is located 1.8 m from the left wall. The whole geometrical picture can be predicted by a three-dimensional simulation.

Figure 11 shows the fire environment inside without actuating the sprinkler, using the field model (Chow and Fong 1991). It is obvious that a stable stratified hot air layer is formed as heat is continuously injected into the enclosure. This is then repeated with the sprinkler water imposed when the ambient temperature is raised to 120°C, *i.e.*, 120 s after turning on the plume. To simplify the situation, the spray sectional pattern is a parabolic hollow surface calculated by the water droplet trajec-

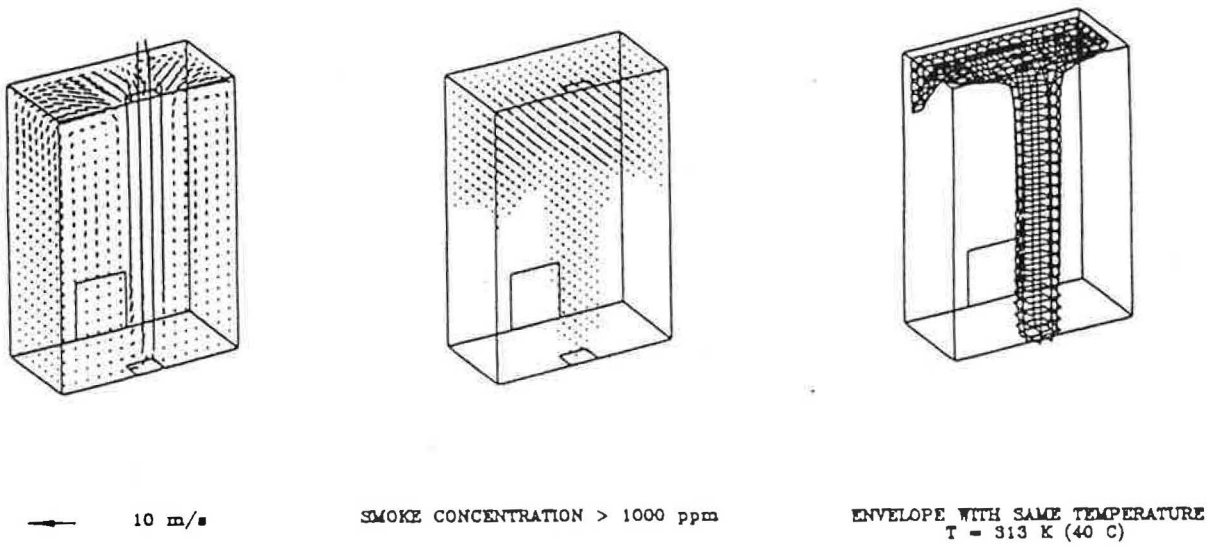

Figure 8 *Flow field, smoke, and temperature distribution for atrium under natural ventilation*

tories as shown in Figure 10. The sprinkler water spray is assumed to be operated with constant initial droplet velocity with components of 4 ms^{-1} in both x and y directions. The total number of droplets inside the water spray is 106 $m^{-1}s^{-1}$, with a mean diameter of 0.6 mm. This is equivalent to a common type of sprinkler head operating at a pressure of 590 kPa and a water flow rate of 1.17 kgs^{-1} as specified in the FOC Rules (1986). The water droplets interact with the fire-induced airflow through convection and dragging effects. In this way, the source terms of the momentum and enthalpy equations in Table 1 are modified. The flow and temperature fields predicted are shown in Figure 11. Note that a steady-state flow pattern results as heat is still injected into the compartment. Heat is confined inside the burning part of the enclosure but downward air movement develops in regions close to the sprinkler. Smoke particulates are brought to the lower part of the compartment, *i.e.*, smoke logging. This illustrates how the fire-induced flow and temperature field would be influenced by a sprinkler water spray. Natural venting seems to be inappropriate if designed adjacent to a sprinkler head.

CONCLUSIONS

The application of field models to fire services design in different examples has been demonstrated. Sizing the capacity of the fan to achieve longitudinal ventilation in order to prevent back layering in tunnels has been demonstrated. Second, the effect of smoke extraction on an atrium building is illustrated. Third, the environment in a sprinklered fire is assessed. These are the key areas for applying the field model in designing appropriate fire safety systems in special buildings.

However, there are weaknesses in this technique. The heat of the released rate of the fire source must be assumed and taken as an input function. This can only be overcome if the combustion effect and thermal radiative feedback from the flame to the fuel can be simulated. Therefore, studying fire at the flashover stage by a field model is sure to be developed (Lockwood and Malalasekera 1988). Another point is the availability of a powerful computer. A three-dimensional simulation must be performed with a good workstation. Finally, only limited experimental data are available for validating a field model and tuning the parameters concerned. These are works that will be developed in future studies and will be reported on later.

ACKNOWLEDGEMENTS

The field model project is funded under a Polytechnic research grant, and the author wishes to thank Dr. A.M. Marsden and Professor H.S. Ward for their encouraging support.

REFERENCES

Baum, H.R.; Reham, R.G.; and Mulholland, G.W. 1982. "Computation of fire induced flow and smoke coagulation." Nineteenth International Symposium on Combustion. Pittsburgh: The Combustion Institute.

Bos, W.G.; Elsen, T. Van Den; Hoogendoorn, C.J.; and Test, F.L. 1984. "Numerical study of stratification of a smoke layer in a corridor." *Combustion Science and Technology*, Vol. 38, p. 277.

Chow, W.K. 1988a. "Sprinkler in atrium building." *The Hong Kong Engineer*, September, pp. 41–43.

Chow, W.K. 1988b. "Application of field models for simulating building fires at the preflashover stage on research note." *The Hong Kong Engineer*, July, pp. 25–27.

Chow, W.K., and Leung, W.M. 1988. "Application of field model to tunnel fire services design." BHRA Sixth International Symposium on the Aerodynamics and Ventilation of Vehicle Tunnels, p. 495. Durham: British Hydromechanics Research Association.

Chow, W.K., and Leung, W.M. 1989. "Fire-induced convective flow inside an enclosure before flashover: Numerical experiments." *Building Services Engineering Research and Technology*, Vol. 10, No. 2, p. 51.

Chow, W.K.; and Fong, N.K. 1990. "Numerical studies on the sprinkler fire interaction using field modelling technique." Proceedings of the Fifth International Fire Conference—Interflam 90, pp. 25–34.

Cox, G., and Kumar, S. 1987. "Field modelling of fire in forced ventilated enclosures." *Combustion Science and Technology*, Vol. 52, p. 7.

Dongarra, J.J. 1987. "Performance of various computers using standard linear equations software in a FORTRAN environment." *Technical Memorandum*, No. 23, Argonne National Laboratory, Chicago.

Fire Officers Committee. 1986. "Rules for sprinkler installation."

Galea, E.R., and Markatos, N.C. 1987. "A review of mathematical modelling of aircraft cabin fires." *Applied Mathematical Modelling*, Vol. 11, p. 162.

Hasemi, Y. 1977. "Numerical calculation of the natural convection in fire compartment." BRI Research Paper No. 69. Tsukuba, Japan: Building Research Institute.

Jones, W.W. 1983. "A review of compartment fire models." NBASIR 83-2684. Gaithersburg: National Bureau of Standards.

Jones, W.W., and Peacook. 1989. "Technical reference guide for FAST version 18." *NIST Technical Note*, No. 1262. Gaithersburg: National Institute of Standards and Technology.

Kumar, S., and Cox, G. 1988. "Radiant heat and surface roughness effects in the numerical modelling of tunnel fires." Proceedings of the Sixth International Symposium on the Aerodynamics and Ventilation of Vehicle Tunnels, pp. 27–29. Durham: British Hydromechanics Research Association.

Launder, B.E., and Spalding, D.B. 1974. "The numerical computation of turbulent flows." *Computer Methods in Applied Mechanics and Engineering*, Vol. 3, p. 269.

Liu, V.K., and Yang, K.T. 1978. "UNDSAFE-11 A computer code for buoyant turbulent flow in an enclosure with thermal radiation. Technical Report TR-79002-28-3, University of Notre Dame, Southbend, IN.

Lockwood F.C., and Malalasekera W.M.G. 1988. "Fire computation: the flashover phenomenon." The Twenty-Second International Symposium on Combustion, pp. 1319–1328.

Mao, C.P.; Fernandez-Pello, A.C.; and Humphrey, J.A.C. 1984. "An investigation of steady wall ceiling and partial enclosure fires." *ASME Journal of Heat Transfer*, Vol. 196, p. 221.

Markatos, N.C., and Cox, G. 1984. Hydrodynamics and heat transfer in enclosures containing a fire source." *Physico Chemical Hydrodynamics*, Vol. 5, p. 53.

Markatos, N.C.; Malin, M.R.; and Cox, G. 1982. "Mathematical modelling of buoyancy-induced smoke flow in enclosures." *International Journal of Heat Mass Transfer*, Vol. 25, p. 63.

Markatos, N.C. 1986. The mathematical modelling of turbulent flows." *Applied Mathematical Modelling*, Vol. 10, p. 190.

Mitler, H.E., and Rockett, H.J.A. 1987. "User's guide to FIRST, A comprehensive single-room fire model." NBSIR 87-3595. Gaithersburg: National Bureau of Standards.

Morgan, H.P. 1979. "Heat transfer from a buoyant smoke layer healther to a ceiling to a sprinkler spray. *Fire and Materials*, Vol. 3, pp. 27–32.

Morgan, H.P. 1991. "A brief historical summary of the 5 MW, 3 m x 3 m design fire used in the United Kingdom for smoke ventilation of shopping malls where there are sprinklers on the retail units." Private communication.

Patankar, S.V. 1980. *Numerical heat transfer and fluid flow.* McGraw-Hill, Washington, D.C.

Porter, A. 1990. "Battersea power station—A study in smoke movement using computational fluid dynamics." Paper presented at the Atrium Engineering Seminar organized by the Institute of Mechanical Engineers, Westminster.

Quintiere, J.G. 1987. "Fundamentals of enclosure fire zone models." National Fire Protection Association Annual Meeting for Society for Fire Protection Engineers, Cincinnati, OH.

Raycraft, J.; Kelleher, M.D.; Yang, H.Q.; and Yang, K.T. 1988. "Fire spread on a three-dimensional pressure vessel." Naval Postgraduate School *Report* NPS-69-88-008.

Rhodes, N. 1989. "Prediction of smoke movement: An overview of field models." *ASHRAE Transactions*, Part 1, pp. 868–877.

Spalding, D.B. 1980. "Mathematical modelling of fluid mechanics, heat transfer, and chemical process: A lecture course." Report HTS/80/1/1980, Imperial College of Science and Technology, London.

Satoh, K. 1983. "Experimental and finite-difference study of dynamic fire behaviours in a cubic enclosure with a doorway." Report No. 55, Fire Research Institute, Tokyo.

Tanaka, T., and Nakamura, K. 1989. "A model for predicting smoke transport in buildings." BRI Report 123. Tsukuba: Building Research Institute.

Thomas, P.H. 1970. "Movement of smoke on horizontal corridors against an air flow." *Institution of Fire Engineers Quarterly*, Vol. 45, pp. 45–50.

Thomas, P.H. 1981. "Fire modelling and fire behaviour in rooms. " Eighteenth International Symposium on Combustion, pp. 503–510.

Van de Leur, P.H.E.; Kleinj, C.R.; and Hoogendoorn, C.J. 1989. "Numerical study of the stratified smoke flow in a corridor. *Fire Safety Journal*, Vol. 14, p. 287.

Waters, R.A. 1989. "Stansted terminal building and early atrium studies." *Journal of Fire Protection Engineering*, Vol. 1, pp. 63–76.

Wichman, I.S., and Baum, H.R. 1988. "An integral analysis of two simple model problems on wind-aided flame spread." *ASME Journal of Heat Transfer*, Vol. 110, p. 437.

Yang, K.T., and Chang, L.C. 1977. "UNDSAFE-1 A computer code for buoyant flow in an enclosure." Report TR-79002-77-1, University of Notre Dame, Southbend, IN.

Yang, K.T.; Loyld, J.R.; Kanury, A.M.; and Satoh, K. 1984. "Modelling of turbulent buoyant flows in aircraft cabins." *Combustion Science and Technology*, Vol. 39, p. 107.

Appendix A

$$a_p = a_{X+} + a_{X-} + a_N + a_S + a_E + a_W + \rho_p \frac{\Delta\tau}{\Delta t} - S_p \qquad ...(A1)$$

$$b = S_c + \rho^*_p \phi^*_p \frac{\Delta\tau}{\Delta t} \qquad ...(A2)$$

ρ^*_p, ϕ^*_p are the values of ρ_p and ϕ_p at an earlier time interval, i.e. $(t - \Delta t)$ with the source term linearized as

$$\int S_f \, d\tau = S_p \phi_p + S_c \qquad ...(A3)$$

and the coefficients are listed as follow

$$a_{X+} = D_{X+} A(|P_{X+}|) + [-F_{X+}, 0] \qquad ...(A4)$$
$$a_{X-} = D_{X-} A(|P_{X-}|) + [F_{X-}, 0] \qquad ...(A5)$$
$$a_N = D_n A(|P_n|) + [-F_n, 0] \qquad ...(A6)$$
$$a_S = D_s A(|P_s|) + [F_s, 0] \qquad ...(A7)$$
$$a_E = D_e A(|P_e|) + [-F_e, 0] \qquad ...(A8)$$
$$a_W = D_W A(|P_W|) + [F_W, 0] \qquad ...(A9)$$

where

$$A(|X|) = [0, (1 - 0.1|X|)^5] \qquad ...(A10)$$

[a, b] : greater value of a and b ...(A11)

$$F_{X+} = (\rho u)_{X+} A_{X+}$$

$$P_{X+} = F_{X+} / D_{X+}$$

$$D_{X+} = \frac{A_{X+} \Gamma_{X+}}{\delta_{X+}} \qquad ...(A12)$$

where P_{X+} is the diffusion coefficient evaluated at the point X+. Similar expressions can be derived for F_{X-}, D_{X-}, etc. The variables are then solved line-by-line by means of the tridiagonal matrix algorithm (TDMA).